International Journal of Applied Pharmaceutics

ISSN- 0975-7058 Vol 17, Issue 1, 2025

Original Article

NETWORK PHARMACOLOGY-BASED COMPUTATIONAL STUDY TO INVESTIGATE THE POTENTIAL MECHANISM OF *SYZYGIUM CARYOPHYLLATUM* AGAINST COLON CANCER

RAMADEVI PEMMEREDDY[1], AJAY MILI[1], BHARATH HAROHALLI BYREGOWDA[2], JYOTHI GIRIDHAR[3], SREEDHARA RANGANATH PAI K.[2], ANNA MATHEW[1], VASUDEV PAI[1], CHANDRASHEKAR K. S.[1]*

[1,2]Department of Pharmacognosy, Manipal College of Pharmaceutical Sciences, Manipal Academy of Higher Education, Manipal-576104, Karnataka, India. [3]Department of Pharmaceutical Chemistry, Manipal College of Pharmaceutical Sciences, Manipal Academy of Higher Education, Manipal-576104, Karnataka, India

*Corresponding author: Chandrashekar K. S.; *Email: cks.bhat@manipal.edu

Received: 28 Aug 2024, Revised and Accepted: 04 Nov 2024

ABSTRACT

Objective: *Syzygium caryophyllatum,* a traditional medicinal plant from the Myrtaceae family, is rich in potential phytoconstituents. Based on its ethnobotanical uses and documented pharmacological activities, present work was conducted to evaluate the probable mechanism of action of *S. caryophyllatum* to manage colon cancer by integrating network pharmacology and computational studies.

Methods: The plant extract was prepared by Soxhlet extraction method and *in vitro* screening was performed using Sulforhodamine (SRB) Assay on HT 29 cancer cell lines. We have used super-PRED database, Cytoscape network analyser tool, string database and CytoHubba for performing network analysis for the extract compounds reported in GC-MS analysis. The Kyoto Encyclopedia of Genes and Genomes (KEGG) pathway and DAVID databases were used for gene set enrichment analysis. We have used Schrödinger suite Version 11.4's to perform computational studies.

Results: The extract has demonstrated significant *in vitro* cytotoxic activity (IC50 value is 49.01 µg/ml) and the GC-MS analysis identified seventy-six distinct compounds. The Gene Ontology (GO) and KEGG demonstrated that the shared targets were strongly associated with key processes involved in colon cancer. The current study has identified Estrogen Receptor Alpha (ESR1), Heat Shock Protein 90 Alpha Family Class A Member 1 (HSP90AA1), Mitogen-activated protein kinase 3 (MAP3K), Epidermal Growth Factor Receptor (EGFR) and Signal transducer and activator of transcription 3 (STAT3) proteins as essential targets and 5,7-Dihydroxy-2-undecyl-4H-chromen-4-one, 7a,12-Dihydroindolo[2,3-a] quinolizine, 5-hydroxy-7-methoxy-2-methyl-8-(3-methylbutyl) chromen-4-one as key compounds. Docking studies of the compounds with core proteins completely supplemented their binding affinity and suggested strong interactions at the binding site.

Conclusion: These outcomes highlight the multi-target, multi-compound, and multi-pathway approaches of *S. caryophyllatum* against colon cancer.

Keywords: *Syzygium caryophyllatum*, GC-MS analysis, SRB assay, Network pharmacology, Molecular docking

DOI: https://dx.doi.org/10.22159/ijap.2025v17i1.52490 Journal homepage: https://innovareacademics.in/journals/index.php/ijap

INTRODUCTION

Cancer is the most commonly occurring disease in the world. In accordance with World Health Organization (WHO) data from 2023 reports, colorectal cancer comes in second in terms of cancer-related fatalities globally, with more than 1.9 million new instances and 930,000 deaths predicted for the disease in 2020. By 2040, there would be 3.2 million new instances of colorectal cancer and 1.6 million deaths annually [1].

The lethality of colon cancer remains a cause for concern, in spite of existence of current therapeutic alternatives, including intensive resection surgeries, radiotherapy, palliative care, neoadjuvant chemotherapies, and intensive laparoscopic surgeries for primary tumors [2, 3]. However natural compounds/agents used as chemotherapeutic medications have shown numerous advantages compared to synthetic ones, mostly due to their lower risk of adverse effects, and greater therapeutic efficacy [4, 5]. Today's most effective and curative anticancer treatments are obtained from plant-based sources. Since the NCI program began, approximately 35,000 plant species have been studied, leading to the development of anticancer medications, including Etoposide analogues, Vincristine, Vinblastine, Camptothecin, Indicine–N-oxide, and Taxol [6].

Syzygium caryophyllatum, belonging to the family Myrtaceae, is a folkloric herb. The tender leaves of this plant have been used traditionally in India to cure wounds, ulcers, diarrhea, and stomatitis [7]. The traditional practitioners in Sri Lanka use this plant for treatment of diabetes mellitus and inflammation [8]. Studies conducted on this plant revealed that the plant has shown antimicrobial activity [9], antidiabetic [10, 11], antioxidant and anticancer activities [12]. The anticancer study conducted on the methanolic extract of *S. caryophyllatum* plant by rohit *et al.* has led to the isolation of few phytocompounds such as 3,7-Dihydroxy-4-methoxy flavones, quercetin, and 6,4 dihydroxy 3'propen chalcone, claimed to possess cytotoxic activity on HeLa cancer cell lines [12], However, It's yet unclear how the therapeutic targets and the beneficial phytoconstituents interact. Additionally, there may be some undiscovered chemical moieties present in the plant that may have anticancer activities.

The current strategy of drug discovery, which focuses on using one medicine to treat one specific ailment, is currently encountering significant problems in terms of safety, effectiveness, and long-term survivability. Bioinformatics advancements have transformed medication design and discovery by integrating network biology and polypharmacology to create medicines targeting multiple diseases. Network pharmacology, a combination of network biology and polypharmacology has evolved as an efficient method for elucidating the pharmacological mechanisms underlying multitarget drugs in a variety of disorders [13, 14].

In the current investigation, the ethanolic extract of *S. caryophyllatum* leaves was screened using the Sulforhodamine (SRB) Assay and then subjected to GC-MS analysis to identify the phytoconstituents. Secondly, we predicted the putative active constituents, associated target genes and the pathways of the compounds against colon cancer by network pharmacology. Finally, we conducted docking and simulation studies to evaluate the therapeutic potential of *S. caryophyllatum* plant constituents in Colon cancer.

MATERIALS AND METHODS

Preparation of ethanolic leaf extract

The leaves of *S. caryophyllatum* were collected from Manipal, Karnataka, India in the month of March to August and authenticated.

The voucher specimen (PP 652) was deposited in Manipal College of Pharmaceutical Sciences, Department of Pharmacognosy. The leaves of the plant *S. caryophyllatum* were shade-dried, coarsely ground, and then extracted using ethanol in a Soxhlet extractor, the excess solvent was extracted and concentrated.

Evaluation of cytotoxic activity by SRB assay

To test the cytotoxicity of the extract, 5,000 cells per well were seeded in 96-well plates using 100 µl media. Following a 24-hour period of cell seeding, the cells were exposed to treatment with extract at various concentrations (500 to 15.62 µg/ml). Meanwhile, cells that were not exposed to any treatment were added with an equivalent volume of media, functioning as the control group. Using the SRB assay, cell growth inhibition was performed following a 48 h incubation period. The cell monolayer formed is coloured for 60 min after being fixed with 10% trichloroacetic acid. Following the incubation period, trichloroacetic acid was removed and the wells were dried after three rounds of washing with distilled water. 100 µl** of 0.057% sulforhodamine B solution in acetic acid (1% v/v) was added, kept in dark for 30 min. 200 µl** of Tris base (10 mmol) was added to the wells to dissolve the dye bound to the protein. A multiplate reader (BioTek Instruments Inc. ELx800) was used to examine the absorbance at 540 nm. The IC50 values were calculated using graph pad prism 7 [15, 16].

GC-MS analysis

GC-MS Analysis of *S. caryophyllatum* extract was analysed using GC/MS Clarus 500 (Perkin Elmer) equipment coupled with Restek Rtx^{R} – 5 column having dimensions of 30 mm X 0.25 mm. The oven temperature was set as follows: 40 degrees Celsius for 5 min, then gradually increased to 280 degrees Celsius after 15 min and the injector was set to 280 degrees Celsius. The chemicals were identified using the National Institute Standard and Technology (NIST) database coupled with the GC-MS instrument.

Prediction of compound targets and colon cancer targets

Total 76 compounds obtained from GC-MS analysis of the extract (after removing the duplicates) are selected for network pharmacology. The probable targets were identified using Super-PRED, an online compound target prediction engine. The PubChem Compound names were used as search input. Uniprot ID mapping tool was then used to match the predicted chemical targets to their standard gene names [17]. Gene Cards database was used to find the Colon cancer target genes using the phrase "Colon cancer" with a relevance score ≥20 [18].

Building a protein-protein interaction (PPI) network

The PPI network was depicted by Cytoscape v3.10.1. and its topological parameters were examined using Cytoscape Network Analyzer tool [19]. Using the String database v2.0.1, the PPI network of shared targets between the active drugs and colon cancer was constructed; a confidence score of 0.7 is determined as the optimum score. The software extension CytoHubba was subsequently employed to compute the hub targets based on network node's topological characteristics and target genes [20].

Gene set enrichment analysis

Enrichment analysis was performed using the Kyoto Encyclopedia of Genes and Genomes (KEGG) pathway (updated 1st May 2021) and DAVID ver. 6.8 was used to perform pathway and functional annotation [21].

Molecular docking studies

Molecular docking investigations were conducted to comprehend the mechanism of binding of the chemical constituents discovered in *S. caryophyllatum* to five hub Colon cancer targets, identified by network pharmacology. For the study, the modules of Schrödinger suite Version 11.4's were utilized.

The co-crystallized protein-ligand complex structures of colon cancer targets namely Estrogen Receptor Alpha (ESR1), Heat Shock Protein 90 Alpha Family Class A Member 1 (HSP90AA1), Mitogen-activated protein kinase 3 (MAP3K), Epidermal Growth Factor Receptor (EGFR), Signal transducer and activator of transcription 3 (STAT3), bearing PDB ID's 5GTR, 4BQG, 2ZOQ, 6VHN and 6NJS, respectively were downloaded from RCSB protein data bank. The protein structure was processed using "protein preparation wizard" in the Schrodinger suite. It consists of subsequent phases: "import and process", "review and modify", and "refine". The missing atoms and the sidechains were substituted using Prime tool during the initial stage, required pH adjustments were made for individual proteins, following this, the hydrogen bonds were optimized and assigned and water molecules larger than 3 Å were eliminated. A low-energy state protein was generated through Restrain minimization utilizing the "OPLS3e (optimization potential for liquid simulation) force field". The energy optimization methodology employed in this stage of protein preparation generates the protein in its most energy-efficient state, thereby facilitating subsequent *in silico* investigations [22]. Utilizing the "Receptor grid generation" interface, a grid representing the chosen protein structures was generated [23]. The structures of the compounds were downloaded from the PubChem database. The "LigPrep" tool was used to prepare ligands. Structures with the lowest energy and associated chirality at pH specific to the proteins were built using the OPLS3e force field. Tautomerization, H-bond addition, ionization Epik, neutralization of charged group, and optimisation of ligand geometry were performed for all the selected ligands [24]. The "Glide module" was utilized for all docking experiments. The Glide module attached prepared ligands on the protein's selected site. In extreme precision (XP) mode, prepared ligands were docked and docking score was calculated [25].

ADME analysis

The docking score, ligand interactions were utilized to determine the five most optimal ligands for each protein. The QikProp tool was used to perform ADME analysis. Using this procedure, the following parameters were established: QPlogPo/w (predicted octanol/water coefficient), QPlogBB (predicted brain/blood partition coefficient), QPlogS (predicted aqueous solubility), QPPCaco (cell permeability), QPlogHERG (cardiotoxicity), and Lipinski's rule of five [26, 27].

Induced-fit docking studies (IFD)

The IFD procedure involved specification of 20 poses for an individual ligand and 0.50 Van der Waals scaling. Energy minimization and estimation of the Prime side chain were subsequently conducted. Every residue in the side chain and ligand conformation was refined to a value of 5 Å. All ligand poses were docked thoroughly, and IFD was determined for each pose [28].

Molecular dynamic simulations (MDS)

Protein-ligand complex dynamics and functionality can often be studied using MDS. Based on the ADME profile, IFD data, and ligand docking score, one compound for each protein will be chosen for MDS. Before starting the MDS, the complete system was submerged in a simple point charge/E solvent model. The counter ions were included to maintain overall electrical neutrality. The buffer box size calculation procedure was applied during the building process; the distance (Å) was a = 10, b = 10, and c = 10, and the corresponding angles were α = 90, β = 90, and γ = 90. The system was configured for MD simulation using the System Builder tool, with the OPLS2005 force field being used constantly throughout the procedure. For system minimization, a minimization tool was employed. Simulation time was set to 100 ns with one frame taken from the trajectory every 100 picoseconds, and 1000 frames produced throughout the process. The NPT ensemble (constant particle number (N), pressure (P) 1.01325 bar, and temperature (T) 310 K) was utilized in the production run, with the force field being OPLS2005. Finally, MDS report was created using the Simulation interaction diagram [29, 30].

RESULTS

SRB assay and GC-MS results

The experimental procedure is depicted in fig. 1. The extract is assessed for cytotoxicity by SRB assay on HT-29 cancer cell lines. The extract has demonstrated a significant and dose-dependent cytotoxic effect (IC50 value of 49.01 µg/ml). The fig. 2 illustrates the viability of HT-29 cell lines following treatment with *S.*

caryophyllatum leaf extract at various concentrations. GC-MS chromatogram of the extract, shown in fig. 3 confirmed the presence of 76 compounds. Table 1 illustrates the names of the compounds, retention times and percentage area.

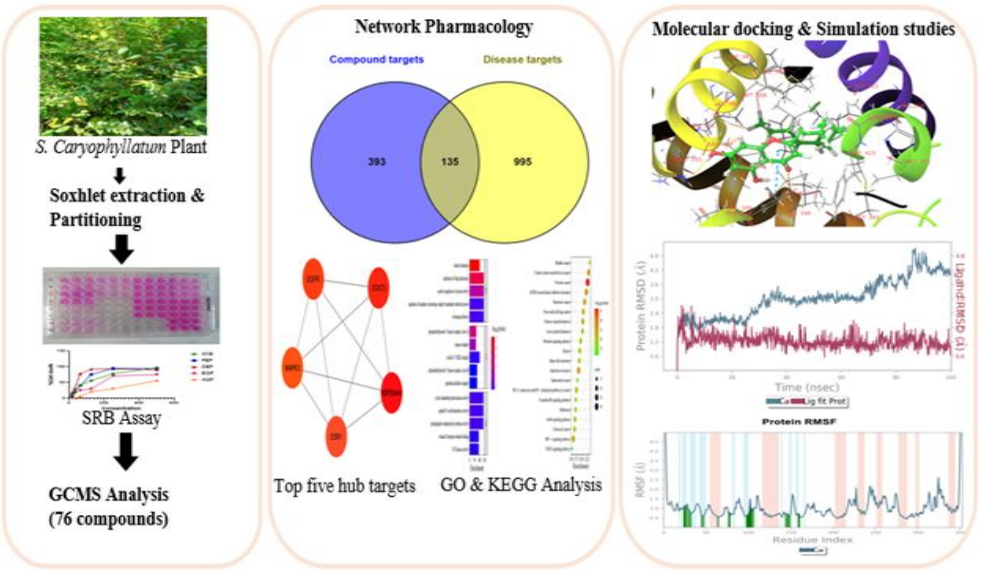

Fig. 1: The framework of study

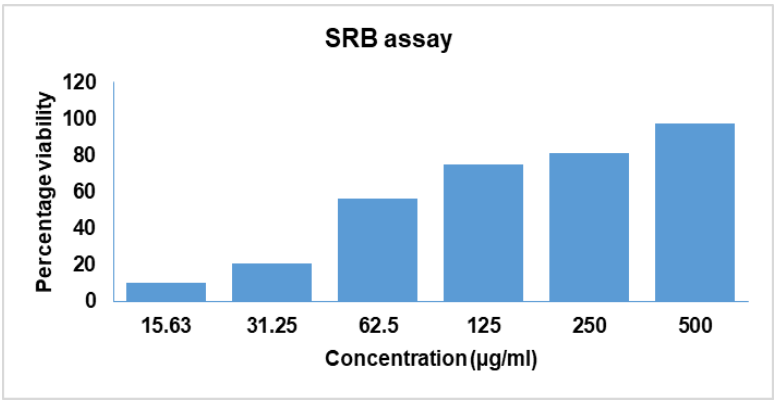

Fig. 2: Cell viability of *S. caryophyllatum* ethanolic extract at various concentrations on HT-29 cancer cell lines

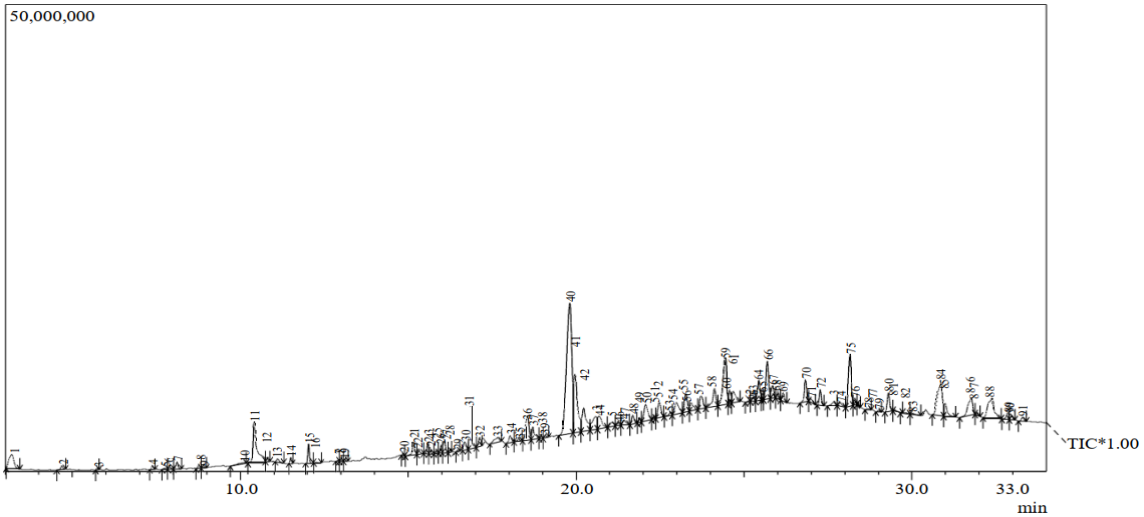

Fig. 3: GCMS Chromatogram of *S. caryophyllatum* leaf extract

Table 1: GC-MS data of *S. caryophyllatum* plant leaf extract

Peak no	Name of the compound	CID	Retention time	Percentage area
1	7-Tetradecenal, (Z)-	CID: 5364468	3.193	1.89
2	Glycerin	CID: 753	4.683	0.26
3	2-Pyrrolidinone, 1-methyl-	CID: 13387	5.746	0.07
4	Ethyl hydrogen succinate	CID: 70610	7.38	0.18
5	5-Hydroxymaltol	CID: 70627	7.738	0.08
6	1,2-Benzenediol	CID: 289	7.887	0.13
7	Benzofuran, 2,3-dihydro-	CID: 10329	8.114	0.39
8	Butanedioic acid, hydroxy-, diethyl ester, (.+/-.)-	CID: 24197	8.757	0.16
9	Malic Acid	CID: 525	8.906	0.07
10	Hexadecanoic acid, 2,3-dihydroxypropyl ester	CID: 14900	10.094	0.24
11	1,2,3-Benzenetriol	CID: 1057	10.4	4.44
12	3,5-Dimethyl-1-dimethylphenylsilyloxybenzene	CID: 532641	10.747	0.24
13	Trehalose	CID: 7427	11.112	0.28
14	5-Isopropenyl-3-isopropyl-2,2-dimethyl-2,5-dihydrofuran	CID: 596568	11.497	0.27
15	Butylated Hydroxytoluene	CID: 31404	12.035	0.88
16	Eicosane	CID: 8222	12.243	0.08
17	1-Chloroeicosane	CID: 39150	12.932	0.06
18	Methyl 9-(2-[(2-butylcyclopropyl)methyl]cyclopropyl)nonanoate	CID: 544392	12.983	0.08
19	N-Methyl-3,5-dihydroxyaniline	CID: 587240	13.115	0.08
20	Tricyclo [3.1.0.0(2,4)] hexane, 3,3,6,6-tetraethyl-, trans--	CID: 572173	14.842	0.07
21	(1E)-2-(2,2,6-Trimethyl-7-oxabicyclo [4.1.0]hept-1-yl)-1-propenyl acetate	CID: 5363712	15.153	0.97
22	2-Cyclohexen-1-one, 4-hydroxy-3,5,6-trimethyl-4-(3-oxo-1-butenyl)-	CID: 5371378	15.309	0.33
23,26,27	cis-9-Hexadecenal	CID: 5364643	15.576, 15.982, 16.078	3.54
24	2-Pentadecanone, 6,10,14-trimethyl-	CID: 10408	15.643	0.3
25	Stigmasta-5,24(28)-dien-3-ol, (3 beta)	CID: 5281326	15.831	0.11
28,31	l-(+)-Ascorbic acid 2,6-dihexadecanoate	CID: 54722209	16.245, 16.837	2.46
29	tert-Hexadecanethiol	CID: 109858	16.457	0.07
30	Cyclopentadecanone, 2-hydroxy-$$ 2-Hydroxycyclopentadecanone	CID: 543400	16.678	0.58
32	Hexadecanoic acid, ethyl ester	CID: 12366	17.123	0.61
33	Cholest-5-en-3-ol (3. beta.)-	CID: 5997	17.663	0.67
34	9-Undecen-2-one, 6,10-dimethyl-	CID: 102604	18.033	0.47
35,36	Phytol	CID: 5280435	18.288, 18.383	0.76
37	Octadecanoic acid	CID: 5281	18.708	0.93
38	Octadecanoic acid, ethyl ester	CID: 8122	18.964	0.09
39	9,12-Octadecadienoic acid (Z, Z)-, 2,3-dihydroxypropyl ester	CID: 5283469	19.076	0.15
40	E, Z-1,3,12-Nonadecatriene	CID: 5365680	19.808	18.41
41	Methyl alpha linolinate	CID: 5319706	19.957	6.04
42, 43	Gamma.-Tocopherol	CID: 92729	20.223, 20.583	4.59
44,54,66, 75	Gamma.-Sitosterol	CID: 457801	20.682, 22.985, 25.689, 28.156	9.6
45	Cholestane-3,6-diol, (3. beta.,5. alpha.,6. alpha.,17. alpha.,20S)-	CID: 22213509	21.054	0.47
46	E, E, Z-1,3,12-Nonadecatriene-5,14-diol	CID: 5364768	21.268, 25.284, 25.846	1.46
47	Linoleoyl-rac-glycerol	CID: 5365676	21.418	0.47
48	Tetracosamethyl-cyclododecasiloxane	CID: 167767	21.682	0.62
49	2,6,10,14,18,22-Tetracosahexaene, 2,6,10,15,19,23-hexamethyl-, (all-E)-	CID: 638072	21.887	0.25
50,57,69	Vitamin E acetate $$ dl-. alpha.-Tocopherol acetate	CID: 2117	22.071, 23.718, 26.16	3.5
51	9-Octadecenoic acid, 1,2,3-propanetriyl ester, (E, E, E)-	CID: 5364673	22.342	0.13
52	Ergost-5-en-3-ol, (3. beta.)-	CID: 5283637	22.477, 24.119	3.19
53	2,6-Heptadienal, 2,4-dimethyl-	CID: 5370098	22.819	0.25
55	Stigmasterol	CID: 5280794	23.269	1.54
56	2H-1-Benzopyran-6-ol, 3,4-dihydro-2,8-dimethyl-2-(4,8,12-trimethyltridecyl)-, [2R-[2R*	CID: 12444418	23.429	0.74
59	Lanosterol	CID: 246983	24.427	4.34
60	Beta.-Tocopherol	CID: 6857447	24.566	0.9
61	Stigmasta-4,22-dien-3. beta.-ol	CID: 15215516	24.681, 27.269	2.05
62	Stigmast-5-en-3-ol, oleate	CID: 20831071	25.152	0.1
64	Alpha-tocopherol-beta-D-mannoside	CID: 597057	25.435	1.5
65	4,4,8-Trimethyl-non-5-enal	CID: 5365831	25.535	0.31
68	Triacontane, 1-bromo-	CID: 521082	26.01	0.41
70	Lupeol	CID: 259846	26.831	1.5
71	Cholestanol	CID: 6665	26.981	0.28
73	Linoleic acid ethyl ester	CID: 5282184	27.671	0.33
74	(R)-(-)-14-Methyl-8-hexadecyn-1-ol	CID: 10944926	27.865	0.26
76	Stigmastanol	CID: 241572	28.296	0.33
77	Fucosterol	CID: 5281328	28.399	0.15
78,81	9,19-cyclolanost-24-en-3-ol, (3 beta)-	CID: 129660864	28.696, 29.484	0.1
79	Dihydrochondrillaterol	CID: 5283639	29.006	0.09
80	12-oleanen-3yl acetate, (3 alpha)-	CID: 45044112	29.297	1.24
82	2,3-Benzocyclododecenedimethanol, 1,2,3,4,5,6,7,8,9,10,11,12,13,14-tetradecahydro-, (2	CID: 569165	29.792	0.13
83	alpha-Amyrin acetate	CID: 293754	30.021	0.12
84	2-Ethyl-4-(2-methylcyclohexyl)-5,6,7,8-tetrahydro-4H-1,3,2-benzodioxaborinine	CID: 609622	30.861	4.59
85	5,7-Dihydroxy-2-undecyl-4H-chromen-4-one	CID: 5375797	30.987	1.03
86	Dihydroindolo[2,3-a] quinolizine	CID: 613040	31.772	2.28
87	4-Methyl-1-(2,6,6-trimethyl-2-cyclohexen-1-yl) pent-1-en-3-one	CID: 5376281	31.93	0.09
88	5-hydroxy-7-methoxy-2-methyl-8-(3-methylbutyl)chromen-4-one	CID: 613101	32.384	3.4
89	2-piperaine-4-amino-6,7-dimethoxyquinaoline	CID: 616267	32.848	0.54
90	D; B-Friedo-B; A-neogammacer-5-en-3-ol, (3-beta)-	CID: 12442794	32.934	0.37
91	Friedelan-3-one	CID: 91472	33.296	0.31

CID: Compound identifier

Network pharmacology analysis

Network Pharmacology has been performed for the 76 chemicals found in the extract and the putative targets of the Colon cancer. The Super-PRED server identified a total of 528 distinct targets from 76 compounds found in the *S. caryophyllatum* plant leaf extract. In the same manner, A total of 1131 targets relevant to colon cancer were found, having a relevance threshold score of 20 or above. A total of 135 overlapping targets between the chemicals and the Colon cancer were determined using an online Venn Diagram tool shown in fig. 4A.

A PPI network was constructed utilizing String Database v2.0.1 to reveal the interactive connection among the 135 shared targets. In the PPI network, all 135 targets displayed interactions with a confidence score exceeding 0.70. In this experimental investigation, the degree of a node denotes the count of its immediate neighbours. It is widely accepted that the influence exerted by a node increases in proportion to the number of nodes that are directly connected to it. Betweenness centrality quantifies the shortest path traversed by a given node between every pair of nodes. Closeness centrality is a metric that quantifies the centrality of a node in a network [31]. A higher number of closeness centrality denotes a greater centrality of node, suggesting that signals are transmitted more quickly from that node to other nodes. As shown in fig. 4B, the degree of interaction between the targets is represented by the distinct colours of the nodes of PPI network (green < blue< yellow), the size of the nodes shows their betweenness centrality, and their shape shows their closeness centrality (Square <hexagon <circle). The network consisted of 135 nodes and 962 edges. The CytoHubba software was used to determine the network's five most important targets, as determined by the degree of interactions, betweenness centrality and closeness centrality; the targets are HSP90AA1, STAT3, EGFR, MAPK3 and ESR1(fig. 4C). Table 2 represents the data values of top five targets of network analysis.

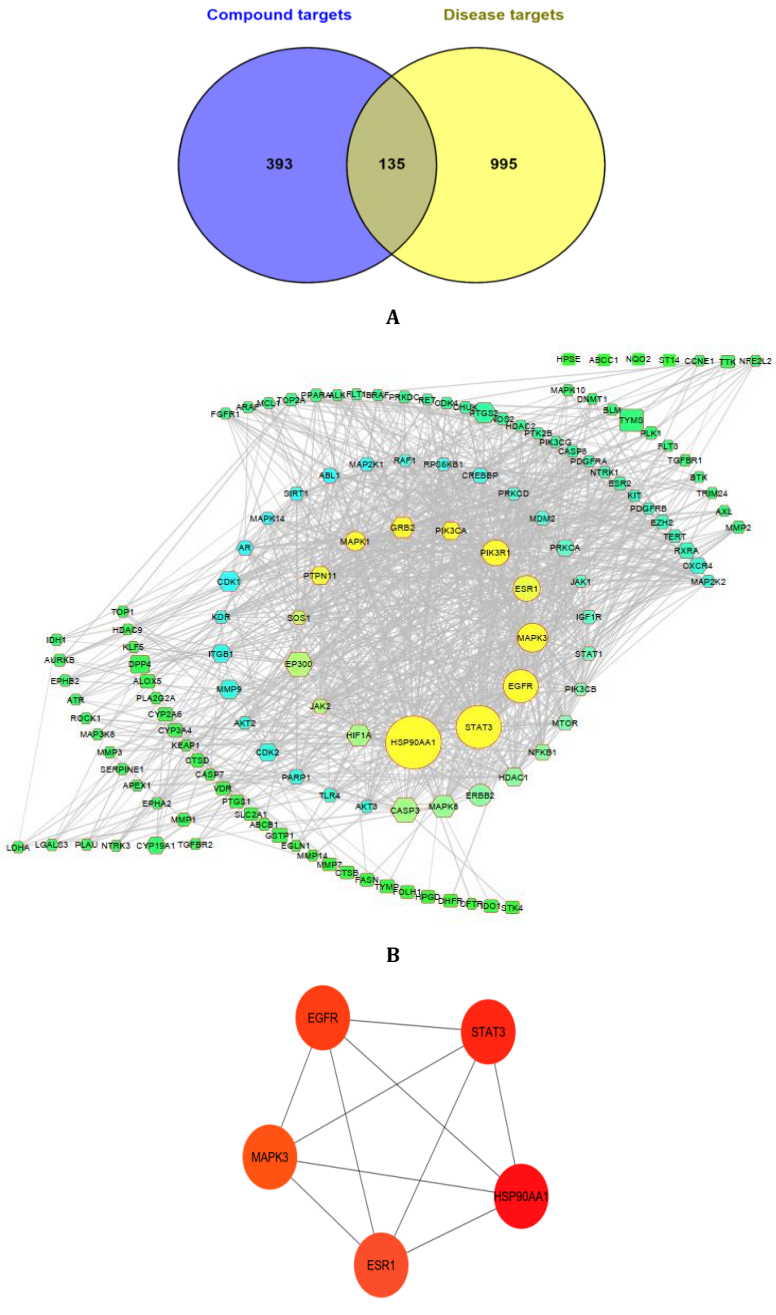

Fig. 4: (A) Venn diagram depicts the most commonly targeted genes for chemical compounds and disease. (B) PPI network of 135 colon cancer targets of *S. caryophyllatum*. (C) The top five targets of PPI networks

Table 2: Data values of top five targets of network analysis

Protein name	Degree	Betweenness centrality	Closeness centrality
HSP90AA1	60	0.12588496	0.610328638
STAT3	55	0.09496326	0.616113744
EGFR	45	0.060568805	0.587777778
MAPK3	45	0.053612779	0.580357143
ESR1	44	0.040844799	0.555555556

The DAVID ver 6.8 database was used to perform GO analysis on 135 gene targets. There were 567 identified biological processes (BP), 86 cell compositions (CC), and 150 molecular functions (MF). Based on fold enrichment values ($P < 0.01$), the top five BP, CC, and MF were chosen and are listed in table 3. BPs were primarily associated with regulation of Golgi inheritance, positive regulation of cyclase activity and control of APC-dependent catabolic process in colon cancer. Phosphatidylinositol 3-kinase (PI3K) complex-class IA caspase complex, cyclin E1-CDK2 complex, PI3K complex-class IB, peptidase inhibitor complex is among the CCs. The MF are primarily involved in cyclin-dependent protein kinase activity, peptide N-acetyltransferase activity, prostaglandin-endoperoxide synthase activity, vitamin D response element binding, JUN kinase activity. The KEGG pathway evaluation of the shared targets identified the specific path in which the common targets are significantly enriched. The top 20 signalling pathways include various cancer-related pathways: prolactin, Vascular endothelial growth factor (VEGF), Fc epsilon RI, Erythroblastic leukaemia viral oncogene homologue (ErbB), Hypoxia-Inducible Factor (HIF-1), and EGFR signalling pathways (table 3).

Table 3: GO and KEGG pathway enrichment analysis of *S. caryophyllatum* compound targets

ID	Category	Description	Fold enrichment	P value	Count
GO: 0060440	GO Biological Process	Trachea formation	102.7195767	7.47e-08	5
GO: 0090170	GO Biological Process	Regulation of Golgi inheritance	143.8074074	1.28e-06	4
GO: 0031281	GO Biological Process	Positive regulation of cyclase activity	143.8074074	1.41e-04	3
GO: 1905784	GO Biological Process	Regulation of anaphase-promoting complex-dependent catabolic process	143.8074074	0.013757	2
GO: 0036269	GO Biological Process	Swimming behaviour	143.8074074	0.013757	2
GO: 0097134	GO Cell Compositions	Cyclin E1-CDK2 complex	101.8469136	0.019366	2
GO: 1904090	GO Cell Compositions	Peptidase inhibitor complex	76.38518519	0.025739	2
GO: 0005944	GO Cell Compositions	Phosphatidylinositol 3-kinase complex, class IB	76.38518519	0.025739	2
GO: 0005943	GO Cell Compositions	Phosphatidylinositol 3-kinase complex, class IA	67.89794239	2.19e-05	4
GO: 0008303	GO Cell Compositions	Caspase complex	65.47301587	8.61e-04	3
GO: 0004666	GO Molecular Functions	Prostaglandin-endoperoxide synthase activity	140.3333333	0.014097	2
GO: 0034212	GO Molecular Functions	Peptide N-acetyltransferase activity	140.3333333	0.014097	2
GO: 0097472	GO Molecular Functions	Cyclin-dependent protein kinase activity	140.3333333	0.014097	2
GO: 0004705	GO Molecular Functions	JUN kinase activity	93.55555556	0.021071	2
GO: 0070644	GO Molecular Functions	Vitamin D response element binding	93.55555556	0.021071	2
hsa05219	KEGG Pathways	Bladder cancer	23.64085	4.82e-16	15
hsa05230	KEGG Pathways	Central carbon metabolism in cancer	23.07797	6.23e-27	25
hsa05215	KEGG Pathways	Prostate cancer	22.64972	7.26e-37	34
hsa01521	KEGG Pathways	EGFR tyrosine kinase inhibitor resistance	22.08474	1.33e-28	27
hsa05212	KEGG Pathways	Pancreatic cancer	21.25603	6.20e-26	25
hsa05223	KEGG Pathways	Non-small cell lung cancer	20.64196	1.84e-23	23
hsa05220	KEGG Pathways	Chronic myeloid leukemia	20.40579	2.17e-24	24
hsa05221	KEGG Pathways	Acute myeloid leukemia	20.2535	3.65e-21	21
hsa04917	KEGG Pathways	Prolactin signaling pathway	19.3855	9.79e-21	21
hsa05214	KEGG Pathways	Glioma	18.95471	1.58e-21	22
hsa05211	KEGG Pathways	Renal cell carcinoma	18.72995	2.12e-19	20
hsa01522	KEGG Pathways	Endocrine resistance	18.46238	2.60e-27	28
hsa05213	KEGG Pathways	Endometrial cancer	17.82574	4.71e-15	16
hsa05235	KEGG Pathways	PD-L1 expression and PD-1 checkpoint pathway in cancer	17.42517	1.26e-22	24
hsa04664	KEGG Pathways	Fc epsilon RI signaling pathway	17.10485	1.13e-16	18
hsa05218	KEGG Pathways	Melanoma	17.05206	1.35e-17	19
hsa04012	KEGG Pathways	ErbB signaling pathway	16.72474	2.87e-20	22
hsa05210	KEGG Pathways	Colorectal cancer	16.53027	3.74e-20	22
hsa04066	KEGG Pathways	HIF-1 signaling pathway	16.00637	1.60e-24	27
hsa04370	KEGG Pathways	VEGF signaling pathway	15.33316	3.20e-12	14

GO: Gene ontology, KEGG: Kyoto encyclopedia of genes and genomes

Molecular docking results

Molecular docking studies were performed to determine the binding affinity of bioactive compounds and the core colon cancer targets. The top five colon cancer target proteins after network pharmacology (5GTR, 4BQG, 2ZOQ, 6VHN and 6NJS) were docked with the 76 compounds of *S. caryophyllatum* plant. A greater negative docking score indicates high binding affinity of the ligand to the target protein [32]. Table 4 illustrates the docking score and the interactions of ligands with the proteins of the top five compounds for top five targets. The amino acids GLU353, ARG394 and HIE524 are the key target residues of estrogen receptor antagonists [33]. The compound5375797 showed the highest docking score of-11.823 kcal/mol and hydrogen bond interactions with GLU353, ARG 394 residues of 5GTR protein. The key residues LEU48, SER52, ASP93, GLY97, LEU107, PHE138, TYR139, TRP162, THR184 present in the

ATPaseN-terminal domain of HSP90AA1 protein form the active site of HSP90AA1 protein [34]. With the residues at the active site, compound 613040 has demonstrated the highest docking score of-10.523 kcal/mol and has established stable H-bond interactions and Pi-Pi interactions. The aminoacids ASP123, MET125, SER170 and ASP184 serves as active sites for MAPK3 inhibitors [35]. The molecule 5375797 forms H-bonds with ASP123, MET125, and ASP184 of the protein 2ZOQ (MAPK3), showed a docking score of-8.130 kcal/mol. The residues THR790, MET793, and CYS797 serve as the active sites for EGFR inhibitors [36, 37]. The compound 5371378 shows hydrogen bonds with THR790 MET793 residues of 6VHN (EGFR) protein. The amino acid residues ARG609, SER611, SER613, SER636, GLU638 present in the SH2 domain of 6NJS protein are the key targets for STAT3 inhibitors [38]. The compound 597057 forms stable H-bond interaction with GLU594, ARG595, SER636 residues with a docking score of-7.542 kcal/mol.

Table 4: Docking score, and interactions of top five compounds for top five target proteins

Protein	Compound id	Docking score (kcal/mol)	Interactions
ESR1 (5GTR)	5375797	-11.823	Hydrogen bond interaction: LEU346, GLU353, ARG 394
	569165	-11.229	Hydrogen bond interaction: GLU353, ARG394, Pi-Pi stacking: PHE404
	5988	-10.286	Hydrogen bond interaction: THR347, GLU353, GLY521, HIE524
	5371378	-8.324	Hydrogen bond interaction: LEU346, ARG204
	5365831	-7.314	Hydrogen bond interaction: ARG394
HSP90AA1 (4BQG)	613040	-10.523	Hydrogen bond interaction: ASP93, PHE 138, Pi-Pi stacking: PHE138 Pi-cation: PHE 138
	5283469	-8.356	Hydrogen bond interaction: ASP54, LYS58, PHE138
	613101	-7.988	Hydrogen bond interaction: TYR139, Pi-Pi stacking: PHE138, TRP162
	616267	-7.603	Pi-Pi stacking: PHE138, Pi-cation: PHE138,
	12444418	-6.757	Water mediated hydrogen bond interaction: SER52.
MAPK3(2ZOQ)	5375797	-8.130	Hydrogen bond interaction: ASP123, MET125, ASP184
	70627	-7.0	Hydrogen bond interaction: GLN122, ASP123, MET125
	613040	-6.164	Hydrogen bond interaction: ASP128, Salt bridge: ASP184
	14900	-4.213	Hydrogen bond interaction: MET125
	587240	-3.177	Hydrogen bond interaction: GLN122, ASP123, MET125
EGFR (6VHN)	613101	-9.302	Hydrogen bond interaction: LYS745, THR790, GLN791, MET793
	5371378	-7.202	Hydrogen bond interaction: THR790, MET793
	569165	-7.026	Hydrogen bond interaction: MET793, Water mediated hydrogen bond interaction: CYS797, ASP800
	5376281	-6.308	Hydrogen bond interaction: MET793
	616267	-6.203	Hydrogen bond interaction: MET793, ASN842, ASP855
STAT3(6NJS)	597057	-7.542	Hydrogen bond interaction: GLU594, ARG595, SER636
	5988	-5.202	Hydrogen bond interaction: LYS591, ARG609, SER636, GLU638
	587240	-4.714	Hydrogen bond interaction: GLN635, SER636, Pi-Pi stacking: TRP623
	1057	-4.095	Hydrogen bond interaction: GLU612, SER613, Pi-cation: LYS591
	13387	-3.023	Hydrogen bond interaction: LYS591, SER636

ADME analysis

Drug-like characteristics and ADME properties are important filtration criteria in the drug-design process, and these properties for the top five compounds for each targetted protein were assessed using QikProp tool of maestro module are shown in tables 5 and 6. According to the predicted data, all of the chosen compounds exhibited favorable human oral absorption and both the H-bond donor and acceptor atoms are within the acceptable range. There were no substantial violations of the Lipinski rule of five, with only two compounds, 7427 and 597057, found to violate the rule. With the exception of compound 7427, the Caco-2 permeability of all the compounds was satisfactory (values > 25). The acceptable range for QPlogBB is-3.0 to 1.2, and these values for all the compounds were witin the range. The compound 12444418 has showed higher QlogKhsa and QlogPo/w than the recommended range, while the acceptable range of QlogKhsa and QlogPo/w is-1.5 to 1.5 and-2.0 to 6.5, respectively. The compounds 12444418 and 597057 has shown lower QlogS values than the acceptable limit of-6.5 to 0.5.

Table 5: ADME analysis of compounds

Compound ID	Molecular weight (g/mol)	Hydrogen bond donor	Hydrogen bond acceptor	Psa	Metab	% Human oral absorption	Rule of five
569165	280.45	2	3.4	44.119	6	100	0
5375797	332.439	1	3	78.349	3	100	0
7427	342.299	6	16.8	186.758	8	100	2
5371378	222.283	1	4.75	75.482	3	85.653	0
5365831	182.305	0	2	38.322	2	100	0
613040	220.273	1	0.5	8.984	2	100	0
5283469	354.529	2	5.4	80.995	6	100	0
613101	276.332	0	3	61.048	4	100	0
14900	330.507	2	5.4	79.764	3	100	0
616267	289.336	3	6	78.823	3	78.408	0
70627	142.111	2	4	79.634	3	70.818	0
587240	139.154	3	2.5	58.879	5	78.44	0
12444418	402.659	1	1.5	28.129	3	100	1
5376281	220.354	0	2	25.854	4	100	0
597057	592.855	4	10	97.374	8	83.757	2
1057	126.112	3	2.25	65.652	3	73.803	0
13387	99.132	0	3	32.942	1	81.208	0

Psa: Polar Surface Area, Metab: Number of possible metabolic reactions

Table 6: ADME characteristics

Compound ID	QPlog Po/w	QPlogS	QPlog HERG	QPP Caco	QP logBB	QPlogKhsa
569165	3.368	-4.4	-3.544	1156.859	-0.53	0.49
5375797	4.867	-6.391	-5.931	376.67	-1.849	0.871
7427	-3.669	-0.134	-2.924	14.831	-2.597	-1.118
5371378	1.498	-2.624	-3.288	616.461	-0.663	-0.203
5365831	3.064	-3.204	-3.505	2039.601	-0.423	0.16
613040	2.792	-2.976	-4.833	7591.505	0.456	0.032
5283469	4.962	-6.328	-5.989	432.399	-2.346	0.592
613101	3.502	-3.651	-4.121	1252.582	-0.58	0.386
14900	4.49	-5.732	-5.73	482.566	-2.264	0.395
616267	1.333	-2.501	-5.188	274.904	-0.163	-0.114
70627	-0.338	-0.521	-2.907	364.597	-0.708	-0.751
587240	0.408	-0.964	-3.47	554.264	-0.668	-0.674
12444418	8.298	-9.538	-5.928	3005.087	-0.863	2.111
5376281	3.97	-4.431	-3.72	4731.596	0.087	0.557
597057	6.096	-7.351	-5.642	424.508	-2.342	0.98
1057	0.093	-0.323	-3.225	387.014	-0.738	-0.812
13387	-0.362	1.015	-1.15	1412.992	0.14	-1.228

QPlog Po/w: Predicted octanol/water partition coefficient, QPlogS: Predicted aqueous solubility, QPlog HERG: Predicted IC50 value for blockage of HERG Kþ channels, QPP Caco: Predicted apparent Caco-2 cell permeability, QP logBB: Predicted brain/blood partition coefficient, QPlogKhsa: Prediction of binding to human serum albumin

IFD analysis

Top five compounds for each protein have been chosen for IFD depending on their interactions with the protein targets docking score. After IFD, the compound 5375797 has been chosen for MD simulation studies for the proteins 5GTR and 2ZOQ, as this compound has shown highest negative IFD score and also retained bonds. The compounds 613040 and 613101 are selected for MD analysis for 4BQG and 6VHN, respectively based on their IFD scores and bond retention. For the protein target 6NJS, MD analysis was not carried out as the compounds did not retain bonds during IFD analysis. The 3D interaction image of the compounds seleced for MD simulation studies are displayed in fig. 5.

Molecular dynamics (MD) simulation study results

The primary goal of MD studies is to subject the receptor-ligand complex to physiologic settings that were not possible with ligand docking or IFD. Four protein-compound complexes (5375795-5GTR complex, 613040-4BQG complex, 5375797-2ZOQ complex, 613101-6VHN complex) were subjected to MD studies. During MDS, a trajectory frame was generated every 100 ps. 1000 frames were generated when MDS was performed for 100 ns. Analysis of "Root mean square deviation (RMSD)," and "Root mean square fluctuation (RMSF)" was also carried out. By aligning generated frames of protein and ligand-protein complex with the reference frame, the RMSD was computed. The plot of RMSD of proteins on the Y-axis indicates that the variations in protein RMSD are in the range of 1-3Å, which is widely acknowledged as a measure of protein stability during the simulation [39]. For complex 5375797-5GTR, some modest and considerable deviations were seen at about 40-45 ns, and the complex remained stable after 90 ns and no significant conformational change was seen (fig. 6A). In 613040-4BQG complex, significant deviations were observed till 20ns, following that, it remained stable throughout the simulation run, with no significant conformational changes seen (fig. 6B). The complex 5375797-2ZOQ exhibited an initial deviation at around 30–45 ns, following that, it remained stable throughout the simulation run, with no significant conformational changes (fig. 6C). The complex 613101-6VHN remains stable throughout the simulation run (fig. 6D).

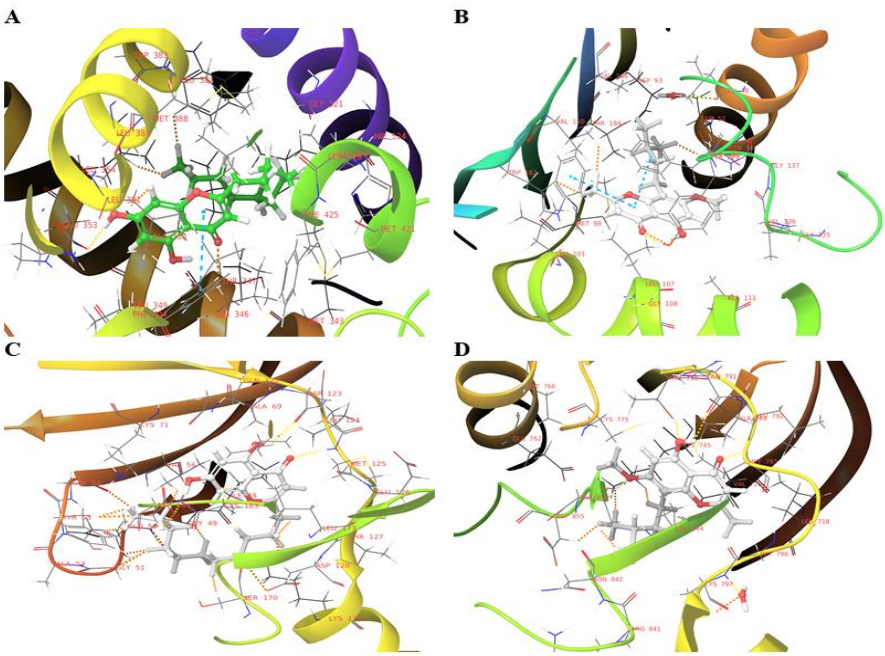

Fig. 5: IFD 3D interaction diagram (A) 5375797-5GTR (IFD score:-487.09), (B) 613040-4BQG (IFD score:-450.20), (C) 5375797-2ZOQ (IFD score:-737.56), (D) 613101-6VHN (-587.54)

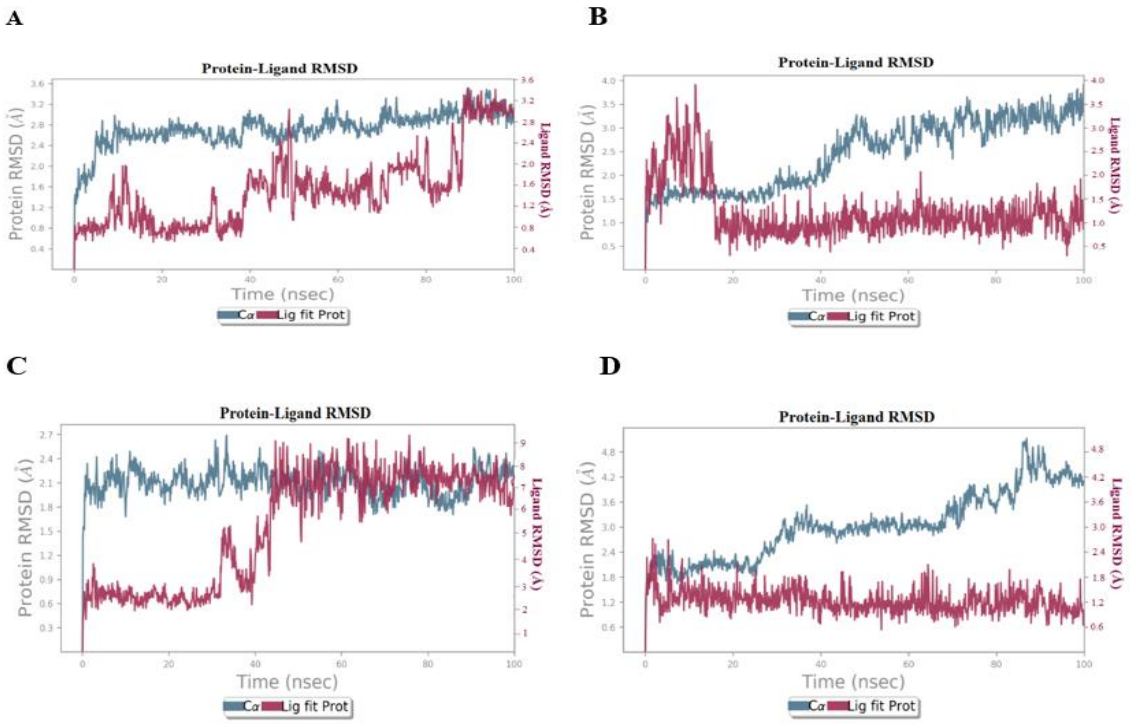

Fig. 6: RMSD Plots (A) 5375797-5GTR complex, (B) 613040-4BQG complex, (C) 5375797-2ZOQ complex, (D) 613101-6VHN complex

RMSF determines the residues responsible for fluctuations in the complexes and illustrates localized variations throughout the protein chain. The RMSF of the protein in relation to all ligands was shown in fig. 7A, 7B, 7C, and 7D. Our analysis revealed that all the four protein-ligand complexes (5375797-5GTR complex, 613040-4BQG complex, 5375797-2ZOQ complex, 613101-6VHN complex) exhibit several regions of significant flexibility, as shown by the peaks in their RMSF profiles. The RMSF values of the interacting residues, represented by green lines, in all the complexes, are below 1.8 Å. This suggests that the interactions formed between the ligands and the proteins are stable.

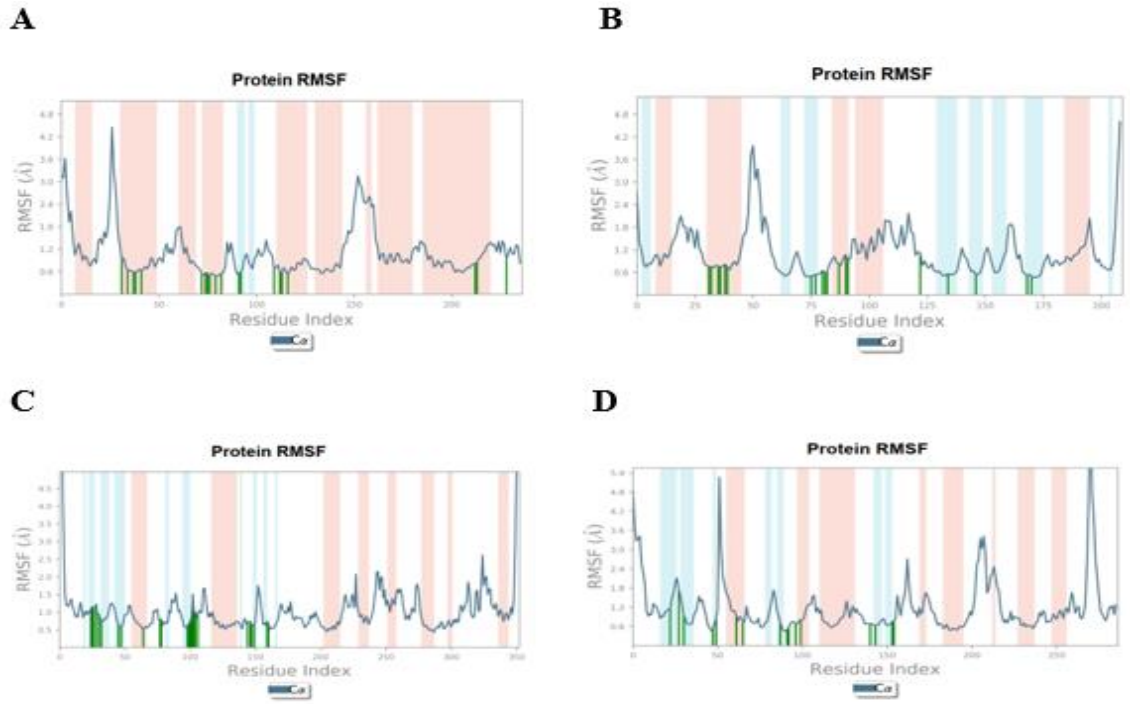

Fig. 7: RMSF Plots (A) 5375797-5GTR complex, (B) 613040-4BQG complex, (C) 5375797-2ZOQ complex, (D) 613101-6VHN complex

The protein-ligand contact pertains to the length of time during which the protein and the ligand interact during MD simulation run. A value of 0.4 signifies that the contact persisted for 40% of the total duration of the simulation, but value higher than 1 implies that there may be

more interactions between the ligand and the protein's amino acid residue. The compound 5375797 demonstrated H-bond interactions with LEU349 and GLU 353 of 5GTR protein, which persisted for 60% and 65% of the simulation run, respectively. The compound 5375797 also formed a pi-pi interaction with PHE 404 residue of 5GTR protein, which lasted for 70% of the simulation run (fig. 8A). Several sustained interactions occurred between compound 613040 and residues TRP 162 and PHE 170 of 4BQG throughout the experiment. Pi interactions were also established between compound 613040 and PHE 138 and TYR 139 of 4BQG for a duration of 65% (fig. 8B). The compound 5375797 shared H-bond interactions with ASP123 and MET125 of 2ZOQ and these interactions lasted for 40% of simulation run. The compound 5375797 had multiple interactions with the residues ASP 184 of 2ZOQ that lasted throughout the experiment (fig. 8C). The compound 613101 formed hydrogen bonds with the key amino acid residues THR 790 and MET 793. These interactions were present for 50% and 100% of the entire simulation duration, respectively (fig. 8D).

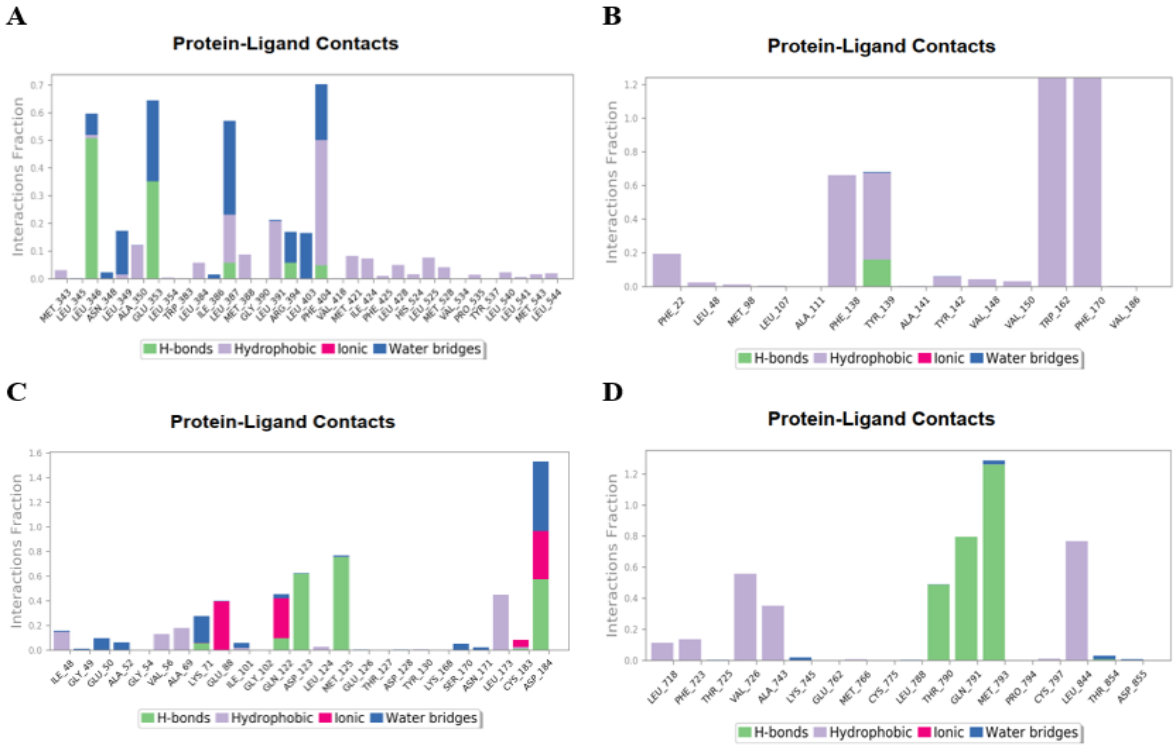

Fig. 8: Histogram of Protein-ligand complex (A) 5375797-5GTR complex, (B) 613040-4BQG complex, (C) 5375797-2ZOQ complex, (D) 613101-6VHN complex

DISCUSSION

Network pharmacology research focuses on the identification of genes associated to compounds and diseases, the building of a PPI network, and the subsequent analysis and visualization of the network [40, 41]. Constructing molecular networks from extensive databases is a straightforward beginning. Subsequently, by employing network analysis, crucial nodes are determined, and essential biological pathways are forecasted [42, 43]. In the current research, we examined the possible molecular mechanisms of the active constituents present in *S. caryophyllatum* leaf extract responsible for its anticancer activity by integrating the network pharmacology and computational approach. *In vitro* cytotoxic assay conducted on the extract revealed that it has shown significant cytotoxic activity against HT 29 cell lines and subsequent GC-MS analysis indicated that the extract contained 76 compounds. The network analysis identified 528 targets of 76 compounds, and a total of 1131 gene targets linked to colon cancer were extracted from the Gene cards database. The Cytoscape software was utilized to identify the five most important hub targets selected based on the degree of interaction, closeness centrality and betweenness centrality and the targets include ESR1, HSP90AA1, MAP3K, EGFR and STAT3. ESR1 is involved in the signalling cascade associated with NOD-like receptors (NLR) in cancer. By inhibiting NLRP3 expression and inflammasome activity, a selective ER antagonist might drastically reduce pro-inflammatory cytokine expression, inhibit cell proliferation, and promote apoptosis [44, 45]. The MAPK pathway is a key target for developing colon cancer therapies. Abnormal MAPK pathway activation in colon cancer can lead to uncontrolled proliferation, resistance to therapy, and the spread of cancer cells to other tissues and organs [46, 47]. According to several studies, MAPK3 overexpression has been linked to the beginning, development and metastasis of several carcinomas, including colon cancer [48]. The HSP90, encoded by HSP90AA1 gene is overexpressed in a number of malignancies, including CRC, and promotes neoplastic transformation by preventing cancer cell invasiveness [49, 50]. Since the discovery of the first Hsp 90 inhibitors, natural compounds have shown enormous potential as a source for creating new inhibitors for Hsp90. As a result, several innovative natural and semi-synthetic HSP90 inhibitors have been developed and are currently being tested in clinical studies [51, 52]. In colitis-associated cancer (CRC), STAT3 over-activates and promotes tumour development, angiogenesis, cancer cell invasion, and migration [53–55].

Our study utilized the KEGG and GO functional enrichment analysis to examine 135 targets. The analysis revealed that the genes are involved in various signalling pathways such as EGFR, PD-L1 expression, Fc epsilon RI, ErbB, HIF-1 and VEGF, which had a role in the development of colon cancers [56]. This suggests that the phytocompounds present in *S. caryophyllatum* plant have a multi-faceted impact on many pathways involved in the genesis of colon cancer.

Furthermore, using the Schrodinger suite Version 11.4 software, an *in silico* docking analysis of the 76 compounds with the target proteins (ESR1, HSP90AA1, MAP3K, EGFR and STAT3) was done to validate the findings of network pharmacology. Further, the results of molecular docking confirmed the presence of a high binding energy between the

selected compounds and the prospective targets. Based on their interactions with the protein targets, docking score, ADME characteristics, IFD score and bond retention, a single compound has been selected for each target protein for simulation studies. The compound 5,7-Dihydroxy-2-undecyl-4H-chromen-4-one (CID: 5375797) was selected for MD simulation research for the proteins 2ZOQ and 5GTR. Based on their IFD scores and bond retention, the compounds 7a,12-Dihydroindolo[2,3-a]quinolizine (CID: 613040) and 5-hydroxy-7-methoxy-2-methyl-8-(3-methylbutyl)chromen-4-one (CID: 613101) are chosen for MD analysis for 4BQG and 6VHN, respectively. The compound 5,7-Dihydroxy-2-undecyl-4H-chromen-4-one (CID: 5375797). The ADME predicted by the QikProp tool indicates that the three compounds (CID: 5375797, CID: 613040 and CID: 613101) adhere to Lipinski's rule of five in terms of druggability, transport properties, and pharmacokinetics. The two compounds 5,7-Dihydroxy-2-undecyl-4H-chromen-4-one and 5-hydroxy-7-methoxy-2-methyl-8-(3-methylbutyl) chromen-4-one are chromone derivatives. Chromones are a type of heterocyclic compounds that include oxygen. Previous research findings show that the chromone derivatives exhibit anticancer activity through a varied array of pathways, including anti-metastasis, cytotoxicity, chemoprevention, anti-angiogenesis, and immune modulation properties [57, 58]. Therefore, to create novel approaches for cancer prevention and treatment, more investigation is necessary to pinpoint the precise molecular pathways underlying the anticancer activity of the bioactive compounds studied in this work.

This study was based on the application of a network pharmacology approach to explore the possible anticancer compounds discovered in the plant *S. caryophyllatum*, an area that had previously been unexplored. Regrettably, the inaccessibility of the compounds for commercial utilization rendered comprehensive *in vitro* and *in vivo* analysis impracticable for our research.

CONCLUSION

The present investigation employed the network pharmacology approach to analyse possible molecular mechanisms of 76 active compounds present in the *S. caryophyllatum* plant leaf extract and the analysis has identified five significant hub target proteins, namely, ESR1, HSP90AA1, MAP3K, EGFR and STAT3. Further Molecular docking studies revealed that the compound 5,7-Dihydroxy-2-undecyl-4H-chromen-4-one docked favourably with the MAPK3 and ESR-1 proteins, the compound 7a,12-Dihydroindolo[2,3-a] quinolizine docked effectively with HSP90AA1 protein, and the compound 5-hydroxy-7-methoxy-2-methyl-8-(3-methylbutyl)chromen-4-one docked with EGFR protein active site. Thus, these findings indicate that the three identified compounds may have a significant role in mitigating colon cancer by affecting the key protein targets that are involved in colon carcinogenesis. Therefore, network pharmacology and computational investigations provide a diverse array of applications and hold immense potential as a strategy for future drug development aimed at reducing the occurrence of colon cancer. Nevertheless, it is crucial to note that further clinical and pharmacological investigation is necessary to substantiate the findings of this study.

ACKNOWLEDGEMENT

All authors express gratitude to Manipal College of Pharmaceutical Sciences (MCOPS) and Manipal Academy of Higher Education (MAHE) for their provision of facilities for this research. The authors express their gratitude to the Manipal-Schrödinger Centre for Molecular Simulations. Ms. Ramadevi Pemmereddy acknowledges the Manipal Academy of Higher Education (MAHE) for providing Dr. T. M. A. Pai Doctoral Fellowship. Mr. Jyothi Giridhar acknowledges the Council of Scientific and Industrial Research (CSIR), Government of India, for providing the Junior Research Fellowship.

FUNDING

Nil

AUTHORS CONTRIBUTIONS

Conceptualization: Ramadevi Pemmereddy and Chandrashekar K. S; Methodology: Ramadevi Pemmereddy and Ajay Mili; Software: Ramadevi Pemmereddy, Bharath Harohalli Byregowda, Jyothi Giridhar and Ajay Mili; Formal analysis: Ramadevi Pemmereddy, Chandrashekar K. S and Sreedhara Ranganath Pai K; Data curation: Ramadevi Pemmereddy, Anna Mathew and Vasudev Pai; Writing-original draft preparation: Ramadevi Pemmereddy and Chandrashekar K. S; Writing, review and editing: Ramadevi Pemmereddy, Ajay Mili, Bharath Harohalli Byregowda and Jyothi Giridhar. All authors have read and agreed to the published version of the manuscript.

CONFLICT OF INTERESTS

The authors confirm that they do not have any competing financial interests or personal relationships that could have impacted the work provided in this study.

REFERENCES

1. World Health Organization. World health statistics 2023: monitoring health for the SDGS sustainable development goals. Available from: https://www.who.int/publications/i/item/9789240074323. [Last accessed on 10 Dec 2023].
2. Kumar A, Gautam V, Sandhu A, Rawat K, Sharma A, Saha L. Current and emerging therapeutic approaches for colorectal cancer: a comprehensive review. World J Gastrointest Surg. 2023 Apr 4;15(4):495-519. doi: 10.4240/wjgs.v15.i4.495, PMID 37206081.
3. Negarandeh R, Salehifar E, Saghafi F, Jalali H, Janbabaei G, Abdhaghighi MJ. Evaluation of adverse effects of chemotherapy regimens of 5-fluoropyrimidines derivatives and their association with DPYD polymorphisms in colorectal cancer patients. BMC Cancer. 2020 Dec;20(1):560. doi: 10.1186/s12885-020-06904-3, PMID 32546132.
4. Wang M, Liu X, Chen T, Cheng X, Xiao H, Meng X. Inhibition and potential treatment of colorectal cancer by natural compounds via various signaling pathways. Front Oncol. 2022 Sep 8;12:956793. doi: 10.3389/fonc.2022.956793, PMID 36158694.
5. Atanasov AG, Zotchev SB, Dirsch VM, International Natural Product Sciences Taskforce, Supuran CT. Natural products in drug discovery: advances and opportunities. Nat Rev Drug Discov. 2021 Mar;20(3):200-16. doi: 10.1038/s41573-020-00114-z, PMID 33510482.
6. Dias DA, Urban S, Roessner U. A historical overview of natural products in drug discovery. Metabolites. 2012 Apr 16;2(2):303-36. doi: 10.3390/metabo2020303, PMID 24957513.
7. Shaikh AM, Shrivastava B, Apte KG, Navale SD. Medicinal plants as potential source of anticancer agents: a review. J Pharmacogn Phytochem. 2016;5(2):291-5.
8. Ediriweera ER, Ratnasooriya WD. A review on herbs used in treatment of diabetes mellitus by Sri Lankan ayurvedic and traditional physicians. Ayu. 2009 Oct 1;30(4):373-91.
9. Shilpa KJ, Krishnakumar G. Nutritional fermentation and pharmacological studies of *Syzygium caryophyllatum (L.) Alston* and *Syzygium zeylanicum (L.) DC* fruits. Cogent Food Agric. 2015 Dec 31;1(1):1018694. doi: 10.1080/23311932.2015.1018694.
10. NS, P SS. Screening of phytochemical and pharmacological activities of *Syzygium caryophyllatum (L.) Alston*. Clin Phytosci. 2018 Dec 1;4(1). doi: 10.1186/s40816-017-0059-2.
11. Rabeque CS, Padmavathy S. Hypoglycaemic effect of *Syzygium caryophyllatum (L.) Alston* on alloxan-induced diabetic albino mice. Asian J Pharm Clin Res. 2013;6(4):203-5.
12. Raj R, Chandrashekar KS, Pai V. *In vitro* anticancer activity of *Syzygium caryophyllatum L*. on hela cell lines using MTT assay. Lat Am J Pharmacol. 2018 Jan 1;37(5):1046-8.
13. Patwardhan B, Chandran U. Network ethnopharmacology approaches for formulation discovery. Indian J Tradit Knowl. 2015;14:574-80.
14. Zhao L, Zhang H, LI N, Chen J, XU H, Wang Y. Network pharmacology a promising approach to reveal the pharmacology mechanism of Chinese medicine formula. J Ethnopharmacol. 2023 Jun 12;309:116306. doi: 10.1016/j.jep.2023.116306, PMID 36858276.
15. Orellana EA, Kasinski AL. Sulforhodamine B (SRB) assay in cell culture to investigate cell proliferation. Bio Protoc. 2016 Nov 5;6(21):e1984. doi: 10.21769/BioProtoc.1984, PMID 28573164.

16. Houghton P, Fang R, Techatanawat I, Steventon G, Hylands PJ, Lee CC. The sulphorhodamine (SRB) assay and other approaches to testing plant extracts and derived compounds for activities related to reputed anticancer activity. Methods. 2007 Aug 1;42(4):377-87. doi: 10.1016/j.ymeth.2007.01.003, PMID 17560325.
17. Omoboyede V, Onile OS, Oyeyemi BF, Aruleba RT, Fadahunsi AI, Oke GA. Unravelling the anti-inflammatory mechanism of *Allium cepa*: an integration of network pharmacology and molecular docking approaches. Mol Divers. 2024 Apr;28(2):727-47. doi: 10.1007/s11030-023-10614-w, PMID 36867320.
18. YU JW, Yuan HW, Bao LD, SI LG. Interaction between piperine and genes associated with sciatica and its mechanism based on molecular docking technology and network pharmacology. Mol Divers. 2021 Feb;25(1):233-48. doi: 10.1007/s11030-020-10055-9, PMID 32130644.
19. Mutiah R, Rachmawati E, Zahiro SR, Milliana A. Elucidating the active compound profile and mechanisms of *Dendrophthoe pentandra* on colorectal cancer: LCMS/MS identification and network pharmacology analysis. J Appl Pharm Sci. 2024 Feb 5;14(2):222-31. doi: 10.7324/JAPS.2024.152900.
20. Sachdeo R, Khanwelkar C, Shete A. *In silico* exploration of berberine as a potential wound healing agent via network pharmacology molecular docking and molecular dynamics simulation. Int J App Pharm. 2024;16(2):188-94. doi: 10.22159/ijap.2024v16i2.49922.
21. Tan S, Yulandi A, Tjandrawinata RR. Network pharmacology study of *Phyllanthus niruri*: potential target proteins and their hepatoprotective activities. J Appl Pharm Sci. 2023 Dec 5;13(12):232-42. doi: 10.7324/JAPS.2023.146937.
22. Gadewar MA, Lal BH. Molecular docking and screening of drugs for 6lu7 protease inhibitor as a potential target for COVID-19. Int J App Pharm. 2022;14(1):100-5. doi: 10.22159/ijap.2022v14i1.43132.
23. Nurhasanah NE, Fadilah FA, Bahtiar AN. Prediction of active compounds of *Muntingia calabura* as potential treatment for chronic obstructive pulmonary diseases by network pharmacology integrated with molecular docking. Int J App Pharm. 2023 Jan 1;15(1):274-9. doi: 10.22159/ijap.2023v15i1.46281.
24. Mili A, Birangal S, Nandakumar K, Lobo R. A computational study to identify sesamol derivatives as NRF2 activator for protection against drug-induced liver injury (DILI). Mol Divers. 2024 Jun;28(3):1709-31. doi: 10.1007/s11030-023-10686-8, PMID 37392347.
25. Mehta SI, Pathak SR. *In silico* drug design and molecular docking studies of novel coumarin derivatives as anticancer agents. Asian J Pharm Clin Res. 2017;10(4):335-40. doi: 10.22159/ajpcr.2017.v10i4.16826.
26. Sahayarayan JJ, Rajan KS, Vidhyavathi R, Nachiappan M, Prabhu D, Alfarraj S. In silico protein-ligand docking studies against the estrogen protein of breast cancer using pharmacophore-based virtual screening approaches. Saudi J Biol Sci. 2021 Jan 1;28(1):400-7. doi: 10.1016/j.sjbs.2020.10.023, PMID 33424323.
27. Suresh AJ, Devi R, Noorulla KM, Surya PR. Insights into thioridazine for its antitubercular activity from molecular docking studies. Int J Pharm Pharm Sci. 2015;7(3):344-6.
28. Bhat NB, Das S, Sridevi BV, H RC, Nayaka S, SN. Molecular docking and dynamics supported investigation of antiviral activity of lichen metabolites of *roccella montagnei*: an *in silico* and *in vitro* study. J Biomol Struct Dyn. 2023 Dec 29;41(21):11484-97. doi: 10.1080/07391102.2023.2180666, PMID 36803674.
29. Vanajothi R, Hemamalini V, Jeyakanthan J, Premkumar K. Ligand based pharmacophore mapping and virtual screening for identification of potential discoidin domain receptor 1 inhibitors. J Biomol Struct Dyn. 2020 Jun 12;38(9):2800-8. doi: 10.1080/07391102.2019.1640132, PMID 31269869.
30. Kumar S, Sharma PP, Shankar U, Kumar D, Joshi SK, Pena L. Discovery of new hydroxyethylamine analogs against 3CLpro protein target of SARS-CoV-2: molecular docking molecular dynamics simulation and structure-activity relationship studies. J Chem Inf Model. 2020 Jun 2;60(12):5754-70. doi: 10.1021/acs.jcim.0c00326, PMID 32551639.
31. Mahgoub MA, Alnaem A, Fadlelmola M, Abo Idris M, Makki AA, Abdelgadir AA. Discovery of novel potential inhibitors of TMPRSS2 and Mpro of SARS-CoV-2 using E-pharmacophore and docking-based virtual screening combined with molecular dynamic and quantum mechanics. J Biomol Struct Dyn. 2023 Sep 22;41(14):6775-88. doi: 10.1080/07391102.2022.2112080, PMID 35997154.
32. Gao Y, Nan Z. Mechanistic insights into the use of rhubarb in diabetic kidney disease treatment using network pharmacology. Medicine. 2022 Jan 7;101(1):e28465. doi: 10.1097/MD.0000000000028465, PMID 35029893.
33. Pang X, FU W, Wang J, Kang D, XU L, Zhao Y. Identification of estrogen receptor α antagonists from natural products via *in vitro* and in silico approaches. Oxid Med Cell Longev. 2018;2018(1):6040149. doi: 10.1155/2018/6040149, PMID 29861831.
34. Brasca MG, Mantegani S, Amboldi N, Bindi S, Caronni D, Casale E. Discovery of NMS-E973 as novel selective and potent inhibitor of heat shock protein 90 (Hsp90). Bioorg Med Chem. 2013 Nov 15;21(22):7047-63. doi: 10.1016/j.bmc.2013.09.018, PMID 24100158.
35. Kinoshita T, Yoshida I, Nakae S, Okita K, Gouda M, Matsubara M. Crystal structure of human mono phosphorylated ERK1 at Tyr204. Biochem Biophys Res Commun. 2008 Dec 26;377(4):1123-7. doi: 10.1016/j.bbrc.2008.10.127, PMID 18983981.
36. Heppner DE, Gunther M, Wittlinger F, Laufer SA, Eck MJ. Structural basis for EGFR mutant inhibition by trisubstituted imidazole inhibitors. J Med Chem. 2020 Apr 3;63(8):4293-305. doi: 10.1021/acs.jmedchem.0c00200, PMID 32243152.
37. Heppner DE, Wittlinger F, Beyett TS, Shaurova T, Urul DA, Buckley B. Structural basis for inhibition of mutant EGFR with lazertinib (YH25448). ACS Med Chem Lett. 2022 Nov 10;13(12):1856-63. doi: 10.1021/acsmedchemlett.2c00213, PMID 36518696.
38. Bai L, Zhou H, XU R, Zhao Y, Chinnaswamy K, Mc Eachern D. A potent and selective small molecule degrader of STAT3 achieves complete tumor regression *in vivo*. Cancer Cell. 2019 Nov 11;36(5):498-511.e17. doi: 10.1016/j.ccell.2019.10.002, PMID 31715132.
39. Patel R, Kumar A, Lokhande KB, Swamy KV, Sharma NK. Molecular docking and simulation studies predict lactyl-CoA as the substrate for P300-directed lactylation; 2020.
40. Zhang Y, Yuan T, LI Y, WU N, Dai X. Network pharmacology analysis of the mechanisms of compound herba sarcandrae (Fufang Zhongjiefeng) aerosol in chronic pharyngitis treatment. Drug Des Devel Ther. 2021 Jun 28;15:2783-803. doi: 10.2147/DDDT.S304708, PMID 34234411.
41. Adrian MF, Lubis MF, Syahputra RA, Astyka R, Sumaiyah S, Yudha Harahap MA. The potential effect of aporphine alkaloids from *Nelumbo nucifera* gaertn. As anti-breast cancer based on network pharmacology and molecular docking. Int J App Pharm. 2024;16(1):280-7. doi: 10.22159/ijap.2024v16i1.49171.
42. Sachdeo R, khanwelkar C, Shete A. *In silico* exploration of berberine as a potential wound healing agent via network pharmacology molecular docking and molecular dynamics simulation. Int J App Pharm. 2024;16(2):188-94. doi: 10.22159/ijap.2024v16i2.49922.
43. LI L, Yang L, Yang L, HE C, HE Y, Chen L. Network pharmacology: a bright guiding light on the way to explore the personalized precise medication of traditional Chinese medicine. Chin Med. 2023 Nov 8;18(1):146. doi: 10.1186/s13020-023-00853-2, PMID 37941061.
44. Sakle NS, More SA, Mokale SN. A network pharmacology-based approach to explore potential targets of *Caesalpinia pulcherima*: an updated prototype in drug discovery. Sci Rep. 2020 Oct 14;10(1):17217. doi: 10.1038/s41598-020-74251-1, PMID 33057155.
45. Fan W, Gao X, Ding C, LV Y, Shen T, MA G. Estrogen receptors participate in carcinogenesis signaling pathways by directly regulating NOD-like receptors. Biochem Biophys Res Commun.

2019 Apr 2;511(2):468-75. doi: 10.1016/j.bbrc.2019.02.085, PMID 30797557.

46. Das PK, Saha J, Pillai S, Lam AK, Gopalan V, Islam F. Implications of estrogen and its receptors in colorectal carcinoma. Cancer Med. 2023 Feb;12(4):4367-79. doi: 10.1002/cam4.5242, PMID 36207986.
47. Urosevic J, Nebreda AR, Gomis RR. MAPK signaling control of colon cancer metastasis. Cell Cycle. 2014 Sep 2;13(17):2641-2. doi: 10.4161/15384101.2014.946374, PMID 25486343.
48. Slattery ML, Lundgreen A, Wolff RK. MAP kinase genes and colon and rectal cancer. Carcinogenesis. 2012 Dec 1;33(12):2398-408. doi: 10.1093/carcin/bgs305, PMID 23027623.
49. Baba Y, Nosho K, Shima K, Meyerhardt JA, Chan AT, Engelman JA. Prognostic significance of AMP-activated protein kinase expression and modifying effect of MAPK3/1 in colorectal cancer. Br J Cancer. 2010 Sep;103(7):1025-33. doi: 10.1038/sj.bjc.6605846, PMID 20808308.
50. Szczuka I, Wierzbicki J, Serek P, Szczesniak Siega BM, Krzystek Korpacka M. Heat shock proteins HSPA1 and HSP90AA1 are upregulated in colorectal polyps and can be targeted in cancer cells by anti-inflammatory oxicams with arylpiperazine pharmacophore and benzoyl moiety substitutions at thiazine ring. Biomolecules. 2021 Oct 27;11(11):1588. doi: 10.3390/biom11111588, PMID 34827586.
51. Lacey T, Lacey H. Linking hsp90's role as an evolutionary capacitator to the development of cancer. Cancer Treat Res Commun. 2021 Jan 1;28:100400. doi: 10.1016/j.ctarc.2021.100400, PMID 34023771.
52. Mitra S, Dash R, Munni YA, Selsi NJ, Akter N, Uddin MN. Natural products targeting Hsp90 for a concurrent strategy in glioblastoma and neurodegeneration. Metabolites. 2022 Nov 21;12(11):1153. doi: 10.3390/metabo12111153, PMID 36422293.
53. Gargalionis AN, Papavassiliou KA, Papavassiliou AG. Targeting STAT3 signaling pathway in colorectal cancer. Biomedicines. 2021 Aug 15;9(8):1016. doi: 10.3390/biomedicines9081016, PMID 34440220.
54. Wei N, LI J, Fang C, Chang J, Xirou V, Syrigos NK. Targeting colon cancer with the novel STAT3 inhibitor bruceantinol. Oncogene. 2019 Mar 7;38(10):1676-87. doi: 10.1038/s41388-018-0547-y, PMID 30348989.
55. Lin HC, HO AS, Huang HH, Yang BL, Shih BB, Lin HC. STAT3 mediated gene expression in colorectal cancer cells derived cancer stem-like tumorspheres. Adv in Digestive Medicine. 2021 Dec;8(4):224-33. doi: 10.1002/aid2.13223.
56. Wan ML, Wang Y, Zeng Z, Deng B, Zhu BS, Cao T. Colorectal cancer (CRC) as a multifactorial disease and its causal correlations with multiple signaling pathways. Biosci Rep. 2020 Mar;40(3). doi: 10.1042/BSR20200265, PMID 32149326.
57. Duan YD, Jiang YY, Guo FX, Chen LX, XU LL, Zhang W. The antitumor activity of naturally occurring chromones: a review. Fitoterapia. 2019;135:114-29. doi: 10.1016/j.fitote.2019.04.012, PMID 31029639.
58. Maicheen C, Phosrithong N, Ungwitayatorn J. Docking study on anticancer activity of chromone derivatives. Med Chem Res. 2013 Jan;22(1):45-56. doi: 10.1007/s00044-012-0009-y.